Numerical Investigation on Effect of Dilute Water Spray on Mean Structure for Gaseous Detonation

Hiroaki Watanabe[1], Akiko Matsuo[1], Ashwin Chinnayya[2],
Ken Matsuoka[3], Akira Kawasaki[3], Jiro Kasahara[3]

[1]Department of Mechanical Engineering, Keio University
3-14-1 Hiyoshi, Kohoku, Yokohama, Kanagawa 223-8522, Japan

[2]Institute Pprime – UPR CNRS 3346
ENSMA, 1 avenue Clément Ader, BP 40109,
86961 Futuroscope-Chasseneuil Cedex, France

[3]Department of Aerospace Engineering, Nagoya University
Furo-cho, Chikusa, Nagoya, Aichi 464-8603, Japan

1 Introduction

Since the discovery of detonation phenomena, detonation attracts a lot of attention in terms of safety hazards and propulsion applications. Detonation is a self-sustaining supersonic combustion wave which consists of a leading shock wave and a reaction zone. A severe damage to people and goods may occur if the detonation happens unintentionally in coalmines or nuclear power plants. Therefore, the knowledge on the initiation and mitigation of the detonation are essential and research on detonation is promoted for safety applications. One of the potential solutions is the use of water spray to suppress the detonation. Boeck *et al*. [1] showed that the existence of water droplet whose Sauter mean diameter (SMD) is 13 μm retards the deflagration to detonation transition for atmospheric stoichiometric hydrogen air mixture and that the detonation propagation speed decreases by 3% compared to the CJ velocity. Also, the experimental study by Niedzielska *et al.* [2] observed the complete detonation extinguishment by water spray whose SMD is 500 μm and indicated the possibility of water spray for detonation quenching.

The knowledge on the detonation in the heterogeneous mixture is of primary importance for the mitigation of the detonation by water spray. One of the researches to clarify the structure for gaseous detonation with water droplets (WDs) in terms of the hydrodynamic thickness was conducted by Jarsalé *et al*. [3]. They performed an experiment to generate new data on gaseous detonation through a C_2H_4-air mixture laden with WDs. The cell size drastically increased and the detonation velocity decreased as compared to the dry CJ velocity. Also, they measured the hydrodynamic thickness by the analysis of the post-shock pressure fluctuations and revealed that the ratio of hydrodynamic thickness over the cell size remains quite constant regardless of the presence of WDs. However, they did not clarify the behavior of WDs and the interaction with the detonation such as their motion and the location of evaporation. The numerical approaches as well as the experimental approach are required to understand the structure of gaseous detonation in heterogeneous mixtures and the behavior of WDs when gaseous detonation propagated through a cloud of WDs. Watanabe *et al.* [4] performed two-dimensional (2D) numerical

Correspondence to: watanabe0204@keio.jp (H. Watanabe)

simulation based on previous experiments of Jarsalé *et al*. to analyze the structure of gaseous detonation via Favre averaged one-dimensional profiles. They observed stable propagation of gaseous detonation in the unburned gas mixture with WDs with small velocity decrease (maximum 3.2%) compared to the CJ speed and change of the cellular structure by addition of WDs in the leaner mixture case as in the experiment. From the Favre average analysis, the evaporation of WDs significantly can be seen to change the structure of gaseous detonation. The evaporation is coupled with the detonation wave. Moreover, the velocity, vorticity and temperature fluctuations downstream of the detonation wave are lowered. Additionally, they reported that the hydrodynamic thickness becomes less than that without WDs when the sound speed for two-phase mixture of which one of the assumptions is velocity equilibrium is used. However, they did not consider droplet breakup and the Favre average analysis was performed on a short computational domain from the interaction with the domain laden with WDs (i.e., 100 mm). Moreover, droplet breakup must play a crucial role in phenomena because smaller droplets are generated, which enhances the interactions between the gaseous phase and WDs such as momentum, evaporation and energy transfer. In addition, the statistical Favre average analysis in time and space is required to obtain more physical insight into the phenomena as in previous studies for turbulent cellular gaseous detonation [5], gaseous detonation in a spatially inhomogeneous reactive medium [6], gaseous detonation with a compressible layer [7]. Therefore, the numerical simulations with droplet breakup and statistical Favre average analysis have to be performed.

In this study, 2D numerical simulations based on Eulerian-Lagragian method that take droplet breakup into account are performed on the gaseous detonation with dilute water spray in order to clarify qualitatively the mean structure of gaseous detonation. Detailed discussion is carried out to analyze the mean structure and the interactions between the gas phase and water spray via statistical Favre averaged one-dimensional profiles from the simulated results. The target gas and droplet conditions in the present study are $2H_2$-O_2-$2N_2$ mixture (initial pressure and temperature are 0.01 MPa and 300 K) with uniform water droplets whose diameter is 15.9 μm and apparent density is 5.5 g/m^3.

2 Numerical method

The detonation propagation in a water spray is related to the two-phase flow of gas and droplets. The Eulerian–Lagrangian method is used to model the gaseous detonation laden with water spray. The gaseous phase is assumed to be a viscous, reactive, compressible, and ideal gas. The governing equations combined with porosity for the gaseous phase are the 2D reactive compressible Navier–Stokes equations, with source terms accounting for chemical reactions and interactions with droplets. The chemical species conservation are H_2, O_2, H, O, OH, H_2O, HO_2, H_2O_2 and N_2. The equation of state for an ideal gas is used to close the system. The hydrogen-oxygen combustion is modelled by a detailed model proposed by Hong *et al*.[8] , which considers 9 species and 20 elementary reactions. The thermochemical species properties are calculated using the NASA thermochemical polynomials [9]. As for the transport properties, a method proposed by Gordon *et al.* [10] is used to estimate the gas viscosity and thermal conductivity, the pure species diffusion coefficients are evaluated using the Chapman–Enskog method. The Wilke method is used to estimate the multi-component gas viscosity and thermal conductivity based on the pure species values.

Particle tracking method is employed to reproduce the droplet motion. The governing equations for droplets are Newton's equation of motion, energy conservation equation, mass conservation equation and number density conservation equation. Because the Biot number in this study is much less than unity, we neglect temperature gradient in the energy equation within the particle. The evaporation and breakup are taken into account. The evaporation of WDs is reproduced by the model by Abramzon *et al*. [11]. Droplet breakup occurs under the assumption that the droplet diameter decreases linearly during the breakup process [12]. The critical Weber number (We_c) and non dimensional total breakup time are modeled following

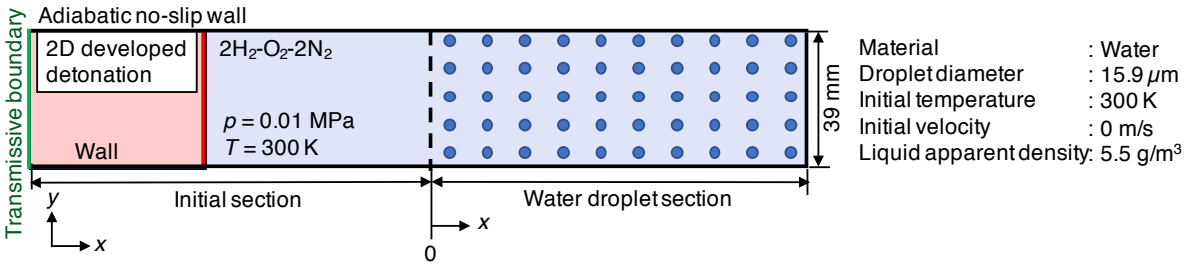

Fig. 1 Computational target

Brodkey [13] and Pilch *et al*. [14]. The drag force is estimated using model proposed by Ling *et al*.[15] and convective heat flux is calculated using the Ranz-Marshall equation.

The convection and diffusion terms are discretized by fifth-order advection upstream splitting methods using pressure-based weight functions (AUSMPW+) improved by Kim *et al*. [16] based on modified weighted essentially non-oscillatory z (MWENO-Z) [17] and the second-order central differential scheme. The time integration method for the convective and diffusion terms is the third-order total-variation-diminishing Runge–Kutta method, and the multi-timescale method [18] is used for efficient time integration of the chemical source term. The time integration of droplet is conducted by the symplectic Euler method. The recycling block method is applied to reduce the computational cost and allows detonation to run a long distance to take statistical value. [7,19,20] In the following calculations, the detonation propagation length is 900 mm.

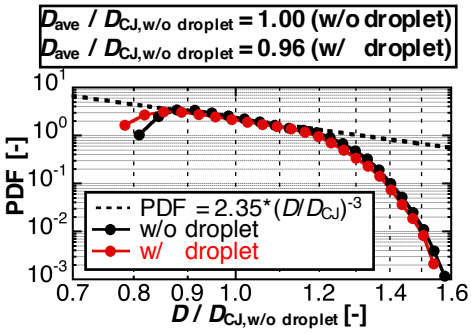

Figure 2 PDF for propagation velocity

3 Results and discussion

The computational target is depicted in Fig. 1. The target gas is 40% N_2 diluted stoichiometric H_2-O_2 mixture and fully developed gaseous detonation propagates through the unburned gas mixture with dilute WDs inside the 39 mm width straight tube. The initial pressure and temperature of gas are 0.01 MPa and 300 K, respectively. The WDs (whose initial diameter and temperature are 15.9 μm and 300 K, respectively) are uniformly distributed in the unburned gas and the apparent density of water is 5.5 g/m^3. The wall is an adiabatic no-slip wall, and a transmissive boundary condition is applied to the left hand side. The half reaction length (*hrl*) is 1696 μm. The minimum grid width is 50 μm and the resolution is about 34 pts/*hrl*. The non-dimensional activation energy for target mixture in the present reaction model is 5.5, and the target gas can be classified as a weakly unstable mixture according to stability analysis [21].

The probability density function (PDF) for propagation velocity is shown in Fig. 2. The gaseous detonation with WDs propagates stably and the decrease in propagation velocity relative to dry CJ velocity without WDs is as much as 4%. The shape of PDF for the case with WDs is the same as that without WDs but shifts to the lower velocity side. The peak in the PDF lies in the sub CJ velocity and the power law dependence assumed from the cylindrical Taylor Sedov blast wave theory is confirmed [5].

The global feature of gaseous detonation with WDs are explained by the 2D flow fields in Fig. 3. Figure 3 shows (a) maximum pressure, (b) gas temperature, (c) droplet volume fraction, (d) evaporation rate, respectively. The maximum pressure corresponds to soot track images. The cellular structure in Fig. 3(a) is regular with 1.5 cell inside the channel. There is no unburned gas pocket in Fig. 3(b). The WDs are locally concentrated behind the shock wave from Fig. 3(c). The evaporation of water droplet occurs after WDs

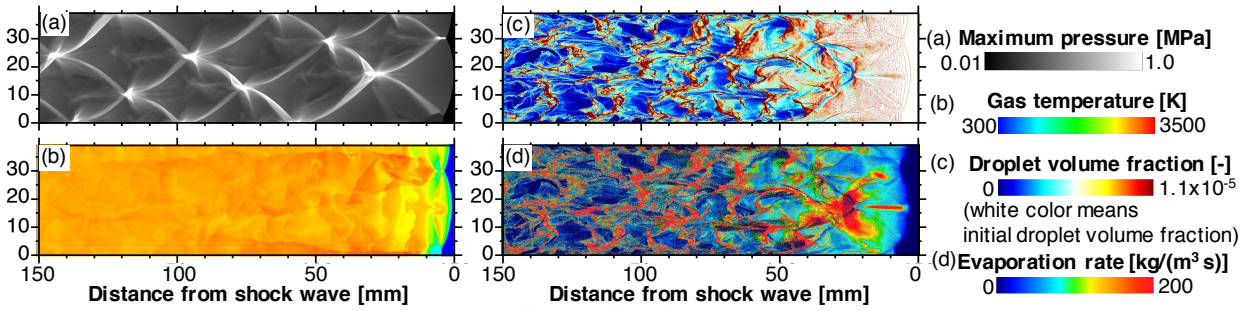

Figure 3 Flow fields

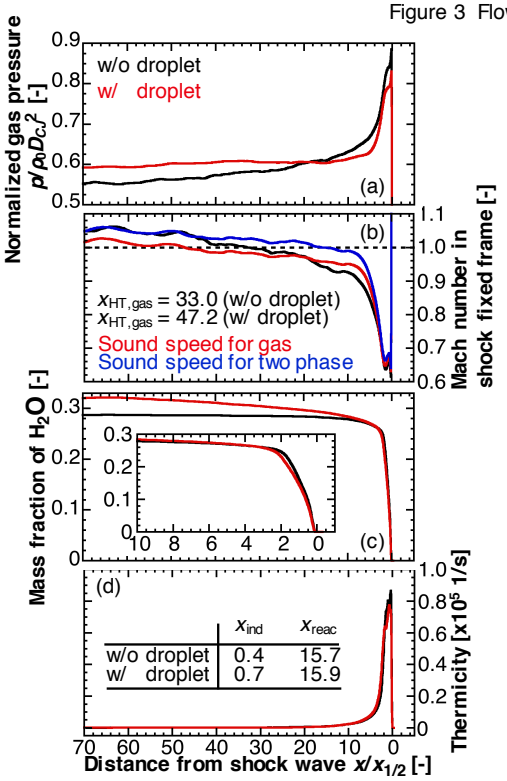

Figure 4 Favre averaged quantity for gas phase

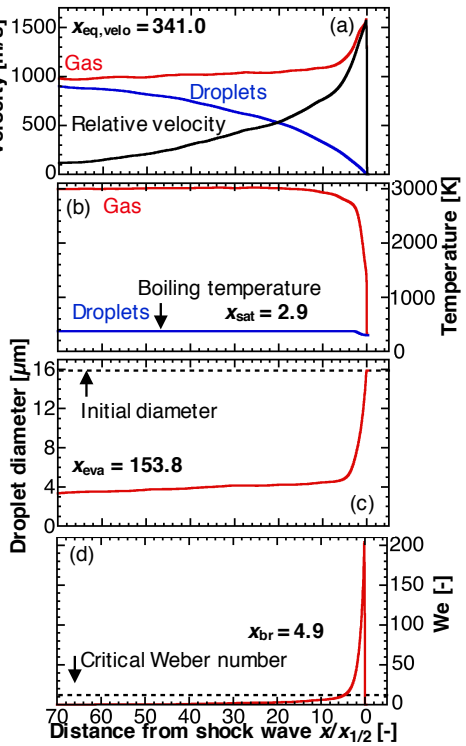

Figure 5 Favre averaged quantity for droplets

reach the boiling temperature in Fig. 3(d), thus mass is transferred to gas phase, whereas heat is taken from the gas.

In order to qualitatively estimate the mean structure of gaseous detonation and the behavior of WDs, the statistical Favre averaging in time and space in the frame of reference of the instantaneous detonation motion is conducted in the simulated results. In order to deal with multiphase features, the Favre averaging process was also applied to the gas density and volume fraction. The WDs are numerically solved based on the Lagrangian method. To obtain Favre averaged one-dimensional profiles for WDs, the physical quantities on WDs (mass, velocity, temperature) are at first projected as the Eulerian grid and then the droplet volume fraction weighted Favre average approach is used. They are shown in Fig. 4 and Fig. 5 for the gas and liquid phases, respectively. Figure 4 shows (a) pressure, (b) estimations of Mach number in shock fixed frame, (c) mass fraction of water vapor H_2O, (d) thermicity and Fig. 5 shows (a) gas and WDs velocities in x direction, (b) gas and WDs temperatures, (c) droplet diameter, (d) We number. As a result of the interaction with WDs, the pressure decreases due to lower propagation velocity as in Fig. 4(a). The sound speed in two-phase medium decreases [22], and the Mach number defined based on the two-phase sound speed and gas phase

sound speed is shown in Fig. 4(b). The hydrodynamic thickness based on gas sound speed $x_{HT,gas}$ with WDs becomes thicker but the hydrodynamic thickness based on two-phase sound speed $x_{HT,two}$ with WDs is shorter than that without WDs. The characteristic lengths for chemical reaction such as induction length x_{ind} and reaction length x_{reac} also become thicker due to the lower propagation velocity in Fig. 4(d). The relative velocity between gas and WDs takes maximum value just behind the shock wave and gradually decreases to the velocity equilibrium. The characteristic length for the velocity equilibrium $x_{eq,velo}$ is defined as the distance from the shock wave to the position where the relative velocity becomes 1% of the maximum value, and estimated as 341.0 *hrl* based on the slope of relative velocity in log scale. The temperature of WDs reaches the boiling temperature soon after the shock wave. The characteristic length for WDs to reach the boiling temperature x_{sat} is then 2.9 *hrl* and is shorter than the characteristic length for velocity equilibrium. The Weber number (We) exceeds We_c downstream of the shock wave and droplet breakup occurs. The characteristic length for breakup x_{br} is defined as the distance from the shock wave and the position where We becomes below We_c in this study and is estimated as 4.9 *hrl* (Fig. 5(d)). Therefore, the droplet breakup ends downstream of the induction zone in the studied case. Indeed, droplet diameter rapidly decreases due to the breakup and then gradually decreases by evaporation as shown in Fig. 5(c). Moreover, the relative velocity decreased due to drag, which contributes to the decrease of the Weber number. The characteristic length for the evaporation is estimated based on the square of droplet diameter history after the breakup finishes and is estimated as 153.8 *hrl*. In order to estimate the influence of the water vapor due to evaporation on the reactivity of the mixture, Fig. 6 shows the Favre averaged Arrhenius, of which slope is the global activation energy. The latter does not change much between the two cases, as the amount of water coming from WDs evaporation within the induction zone is small (see Figs. 4(c), 4(d), 5(d)). Therefore, the increase of the reaction characteristic length is mainly due to the decrease in the detonation velocity. This is due to the interphase exchanges between the gaseous and the dispersed liquid phases, which occur mainly between the leading shock and the mean sonic plane. The different terms in the Favre averaged gaseous total energy are depicted in Fig. 7. Each term decreases due to the interaction with WDs. The peak value for mechanical and thermal fluctuations is the same as that without WDs but the level of the fluctuations diminished with the interaction with WDs presence. From the above analysis, the characteristic lengths of detonation and interphase exchanges can be ordered as follows : $x_{ind} < x_{sat} < x_{br} < x_{reac} < x_{HT} < x_{eva} < x_{eq,velo}$.

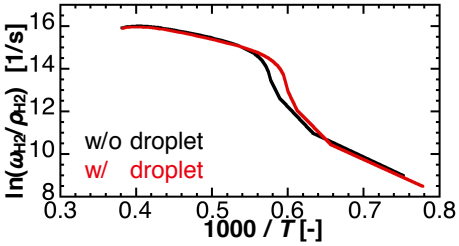

Figure 6 Favre averaged Arrhenius plot

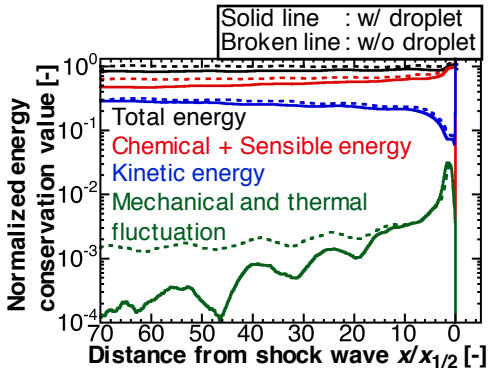

Figure 7 Terms in Favre averaged gaseous total energy conservation

4 Conclusions

In this study, the mean structure of gaseous detonation with dilute water spray is analyzed by 2D numerical simulations under present simulation conditions. The mean structure of gaseous detonation with dilute water spray shares similar structure with gaseous detonation without water spray, and the hydrodynamic thickness of the detonation is changed due to the interaction with water spray. The global two-phase exchanges (mass, momentum and energy exchanges) induce a decrease of the detonation velocity

within the hydrodynamic thickness. Droplet breakup occurs downstream of the induction zone and in our case, the water vapor from the evaporation of water spray does not affect the reactivity of gaseous detonation. The characteristic lengths of detonation and interphase exchanges have been ordered and have been shown to be intimately intertwined.

Acknowledgment

This work is partially supported by "Joint Usage/Research Center for Interdisciplinary Large-scale Information Infrastructures" and "High Performance Computing Infrastructure" in Japan (Project ID: jh170040, jh180030 and hp170039). Some of the simulated results in this research were obtained using supercomputing resources at Cyberscience Center, Tohoku University. An Academic visit of Ashwin Chinnayya to Keio University as Guest Professor (Global) was made possible through a funding for top Global University Project in the Keio University.

References

[1] L. R. Boeck, A. Kink, D. Oezdin, J. Hasslberger, T. Sattelmayer, Int. J. Hydrog. Energy, 40, (2015) 6995-7004

[2] Urszula Niedzielska, Lukasz Jan Kapsta, Bruno Savard, Andrzej Teodorczyk, J. Loss Prevention in the Process Industries, 50 (2017), 229-236

[3] G. Jarsalé, F. Virot, A. Chinnayya, Shock Waves, 26 (2016) 561-572

[4] H. Watanabe, A. Matsuo, K. Matsuoka, A. Kawasaki, J. Kasahara, Proc. Combust. Inst, 37 (2018)

[5] Matei I. Radulescu, Gray J. Sharpe, Chung K. Law, John H. S. Lee, J. Fluid Mech. 580, (2007), 31-81

[6] XiaoCheng Mi, Andrew J. Higgins, Hoi Dick Ng, Charles, B. Kiyanda, Nikolas Nikiforakis, Phys. Review Fluid, 2 053201 (2017)

[7] Maxime Reynaud, Florent Virot, Ashwin, Chinnayya, Phys. Fluids. 29, 056101 (2017)

[8] Zekai Hong, David F. Davidson, Ronald K. Hanson., Combut. Flame, Vol. 158, (2011) 633-644

[9] Bonnie J. McBride, Sanford Gordon, Martin A. Reno, NASA Technical Memorandum 4513, (1993)

[10] Snaford Gordon Bonnie J. McBride, Frank J. Zeleznik, NASA Technical Memorandum 86885, (1984)

[11] B. Abramzon, W. A. Sirignano, Int. J. Heat Mass Transf, 32, (1989) 1605-1618

[12] A. Chauvin, E. Daniel, A. Chinnayya, J. Massoni, G. Jourdan, Shock waves, 26 (2016) 403-415

[13] Brodkey R. S, The Phenomena of Fluid Motions, Addison-Wesley, Reading Mass, 1967

[14] M. Plich, C. A. Erdman, Int. J. of Multiphase Flow, 13, (1987) 741-757

[15] Y. Ling, J. L. Wagner, S. J. Beresh, S. P. Kearney, S. Balachandar, Physics of Fluid, 24, 113301, 2012

[16] Kyu Hong Kim, Chongam Kim, Oh-Hyun Rho, J. Comput. Phys. 174, (2001) 38-80

[17] F. Acker, R. B. de, R. Borges, B. Costa, J. Comput. Phys. 313 (2016) 726-753

[18] Gou X., W. Sun, Z. Chen, Y. Ju, Combust. Flame 157 (2010) 1111-1121

[19] Aliou Sow, Ashwin Chinnayya, Abdellah Hadjadj, J. Fluid Mech. 743 (2014), 503-533

[20] Aliou Sow, Ashwin Chinnayya, Abdellah Hadjadj, Comput. Fluid, 179 (2019) 449-458

[21] Joanna M. Austin, PhD thesis, California Institute of Technology, 2003

[22] Christopher E. Brennen, Cambridge University Press, 2005